Available online at www.sciencedirect.com
ScienceDirect
European Journal of Pharmacology 559 (2007) 124–131
www.elsevier.com/locate/ejphar

Ability of carbazole salts, inhibitors of Alzheimer β-amyloid fibril formation, to cross cellular membranes

Chantarawan Saengkhae [a], Milena Salerno [a,*], Dominique Adès [b], Alain Siove [b], Laurence Le Moyec [a], Véronique Migonney [b], Arlette Garnier-Suillerot [a]

[a] *Laboratoire de Biophysique Moléculaire, Cellulaire et Tissulaire (BioMoCeTi), UMR CNRS 7033, Université Paris 13 et Paris 6, 74 rue Marcel Cachin, 93017 Bobigny, France*
[b] *Laboratoire de Biomatériaux et Polymères de Spécialité, LBPS/B2OA — UMR CNRS 7052, Université Paris 13, 99 Avenue Jean-Baptiste Clément 93430 Villetaneuse, France*

Received 20 October 2006; received in revised form 3 January 2007; accepted 8 January 2007
Available online 19 January 2007

Abstract

Alzheimer's disease is characterized by the presence of β-amyloid fibril formation. The inhibition of this peptide accumulation may be a prevention method for Alzheimer's disease. Several classes of molecules have been reported to inhibit β-amyloid fibril formation and among them carbazoles. However, very few studies have been performed to determine the destination of such molecules *in vivo* and especially if they can pass the blood brain barrier. The aim of this paper is to study whether carbazoles could pass the blood brain barrier, i.e. if they can circumvent ATP Binding Cassette (ABC) transporters such as P-glycoprotein (P-gp) and Multidrug Resistance-associated protein (MRP1) which efficiently limit drug brain uptake. For this purpose we have synthesized a fluorescent derivative of carbazole benzothiazolium iodide 1,2 disubstituted ethylene (referred as carbazole thiazole: CT), which can be easily detected and followed in the pre-trial study phases in cells or in tissue. We use cellular models overexpressing P-gp and MRP1. Our results show that: i) CT is able to cross membranes and to penetrate rapidly inside the cells, ii) CT is a P-gp substrate and consequently its accumulation in P-gp overexpressing cells is very low, iii) CT is a poor MRP1 substrate. In addition once inside the cells, CT rapidly binds to DNA and is then slowly reduced by intracellular reducing agents. In conclusion, the efficiency of carbazole derivatives in inhibiting the β-amyloid formation *in vivo* could be highly compromised because, as P-gp substrates, they will probably not cross the blood brain barrier.

Keywords: Alzheimer; Blood brain barrier; β-amyloid; Inhibitor; Carbazole; P-glycoprotein; MRP1; Membrane

1. Introduction

β-amyloid fibril formation and accumulation in the brain is one of the main features of Alzheimer's disease as well as the neurofibrillar degeneration (Chang and Silverman, 2004). It was shown that the inhibition of this peptide accumulation may be a way for preventing Alzheimer's disease. Several series of compounds inhibiting efficiently β-amyloid fibril formation have been reported (Gianni et al., 1995; Camilleri et al., 1994; Sadler et al., 1995; Wood et al., 1996; Salomon et al., 1996; Tomiyama et al., 1996; Howlett et al., 1997; Sastre et al., 2004; Yang et al., 2005). Among them are carbazole-type compounds (Howlett et al., 1999). These molecules have been mainly studied *in vitro* but the possibility that they can be used *in vivo* has not yet received much attention. Furthermore, the study of the behaviour of such molecules with respect to their transport and destination inside the cells is a major point and a pre-requisite for further studies.

Potential inhibitors of Alzheimer β-amyloid fibril formation have to penetrate into the cerebral tissue. The transport of most compounds from blood to brain is restricted by the presence of the blood brain barrier. Three type of cells are involved in this barrier: endothelial cells of brain capillaries, astrocytes and pericytes (Ballabh et al., 2004). Particular properties of endothelial cells produce this barrier effect: they present more complex tight junctions than in other capillary endothelia and express in their membranes efflux transporters (Abbott, 2002).

* Corresponding author. Tel.: +33 1 48 38 77 48; fax: +33 1 48 38 88 88.
E-mail address: m.salerno@smbh.univ-paris13.fr (M. Salerno).

0014-2999/$ - see front matter © 2007 Elsevier B.V. All rights reserved.
doi:10.1016/j.ejphar.2007.01.005

These membrane proteins function as pumps which extrude exogenous compounds out of the brain tissue. Two of these membrane proteins are the P-glycoprotein (P-gp) and Multidrug Resistance-associated Protein (MRP1) (Amakrishnan, 2003). Both transporters belong to the ATP binding cassette (ABC) protein family, P-gp is also called ABCB1 and MRP1, ABCC1 (Leslie et al., 2005).

In order to test the ability of one class of β-amyloid fibril formation inhibitors, carbazole, to go through the blood brain barrier we have synthesized carbazole thiazole (CT), a red fluorescent salt of carbazole. This fluorescent molecule shows a maximum emission peak around 590 nm. It makes the agent easily detected and followed in the pre-trial study phases in cells or in tissues. To follow the accumulation of this compound inside cells, we used cellular models overexpressing P-gp and MRP1, two proteins overexpressed in blood brain barrier. We show that CT is able to penetrate into cells. However, it is a P-gp substrate which probably compromises its ability to cross the blood brain barrier.

2. Materials and methods

2.1. Drugs and chemicals

Carbazole thiazole (CT) was synthesized using the Knoevenagel condensation between *N*-ethyl-2-methyl benzothiazolium iodide (compound A) and *N*-ethyl-carbazole-3-carbaldehyde (compound B) (Aldrich, Saint Quentin Fallavier, France) according to the reaction scheme described in Fig. 1. The compound A was prepared at 110 °C, in a sealed tube, during 18 h, by quaternization of 2-methyl benzothiazole (Aldrich, Saint Quentin Fallavier, France) by a two-fold excess of ethyl iodide

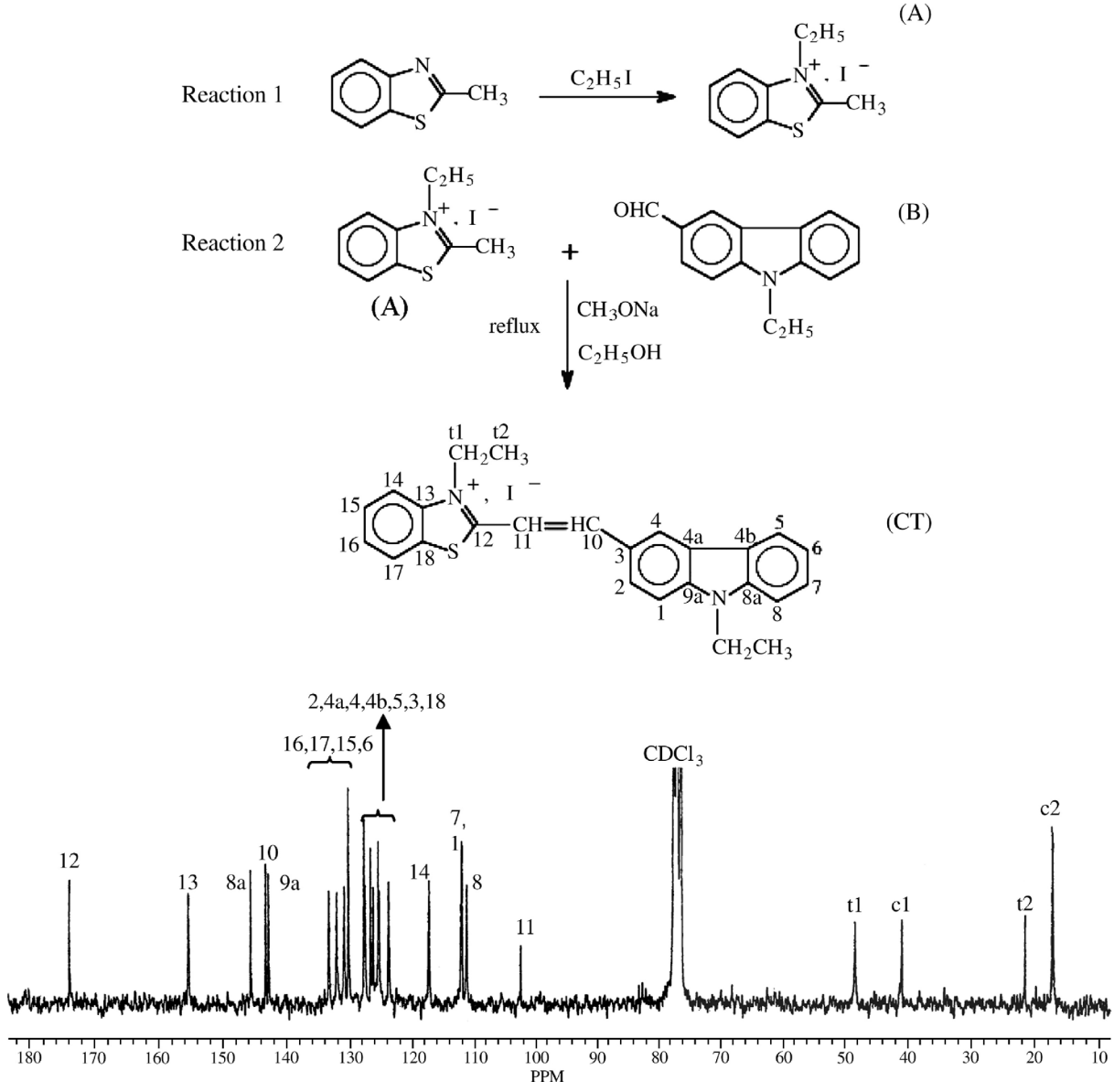

Fig. 1. Synthesis scheme used to obtain the carbazole thiazole (CT) and ^{13}C NMR spectrum obtained at 50 MHz in $CDCl_3$. (A) *N*-ethyl-2-methyl benzothiazolium iodide and (B) *N*-ethyl-carbazole-3-carbaldehyde.

(reaction 1, Fig. 1). The compound A was recovered as bluish needles after recrystallization in hot water with a yield of 70%. In a second step (reaction 2, Fig. 1), the Knoevenagel carbonyl-methylene condensation between A and B was achieved using reflux for 1 h in ethyl alcohol in the presence of sodium methylate as a catalyst. The resulting 1-(*N*-ethyl-2-benzothiazolium iodide)-2-(*N*-ethyl-3-carbazole) ethylene (CT) was obtained as bright red crystals after recrystallization in chloroform, with a yield of 82%. Both the ^{1}H and ^{13}C NMR spectra of CT are in agreement with the expected structure. The 50 MHz ^{13}C NMR spectrum in deuterated chloroform, is shown in Fig. 1 with the spectral assignments. Pure CT was dissolved in water and the concentration was determined by U.V.-visible absorption spectroscopy with $\varepsilon 450 = 24\ 300\ M^{-1}cm^{-1}$. The fluorescence spectrum of aqueous solution of CT exhibits a signal at around 590 nm within the red region of the visible domain.

FCCP and verapamil were purchased from Sigma (Saint Quentin Fallavier, France). They were dissolved in ethanol. The 2-[4-(diphenylmethyl)-1-piperazinyl]ethyl-5-(*trans*-4,6-dimethyl-1,3,2-dioxaphosphorinan-2-yl)-2,6-dimethyl-4-(3-nitrophenyl)-3-pyridinecarboxylate P oxide (PAK-104P) was a gift from Drs. Shudo, Iwasaki and Akiyama (Nissan Chemical Industries, LTD, Japan). Experiments were performed in Hepes buffer containing 20 mM Hepes, 132 mM NaCl, 3.5 mM KCl, 1 mM $CaCl_2$, 0.5 mM $MgCl_2$ at pH = 7.3, with or without 5 mM glucose. All the reagents were of the highest quality available and deionized double-distilled water was used throughout the experiments.

Calf-thymus DNA (Aldrich) was used without purification. The concentration was given by absorption spectra with ε_{260} = 13200/base pair.

2.2. Cell lines and cultures

Two cell lines were used: K562 and GLC4. The K562 cell line is a highly undifferentiated erythroleukemia originally derived from a patient with chronic myelogenous leukemia (Lozzio and Lozzio, 1975). The GLC4 cell line was derived from pleural effusion of a patient with small cell lung carcinoma (Zijlstra et al., 1987). The K562 leukemia cells and the P-gp expressing K562/ADR cell were obtained from Prof. J.P. Marie (Hopital Hotel-Dieu, Paris, France). The GLC4 and the MRP1-expressing GLC4/ADR cells were obtained from Prof. E. G. E. de Vries (Department of Internal Medicine, University Hospital, Groningen, The Netherlands). The K562 and GLC4 cells were cultured in RPMI 1640 Medium with GlutaMAX™I (GIBCO) medium supplemented with 10% fetal calf serum (GIBCO) at 37 °C in a humidified incubator with 5% CO_2. The resistant K562/ADR and GLC4/ADR cells were cultured with 400 nM or 1.2 μM doxorubicine respectively until three weeks before experiments. Cultures initiated at a density of 10^5 cells/mL grew exponentially to about 10^6 cells/mL in 3 days. In order to have enough cells in the exponential growth phase for assay, culture was initiated at 5×10^5 cells/mL and allowed to grow for 24 h until use. Cultured cells were counted with a Coulter counter before use. The viability of the cells, tested by Trypan Blue exclusion, was always greater than 95%.

2.3. Cell nucleus isolation

Cells (10^6/mL) were suspended in Hepes buffer and sonicated in a cold bath 3 times for 30 s (50 HZ, 117 v and 80 W) (Vibra Cell, Sonics and Materials Inc., Danbury, CT). Nuclei were separated form other organelles in the cell by low speed centrifugation and further purified by repeated washes in the same buffer (Farrell, 1998).

2.4. Cellular energy depletion

For energy depletion, cells were incubated for 30 min in a Hepes buffer in which glucose was substituted by 2-deoxyglucose, in the presence of 10 mM sodium azide (NaN_3) (Marbeuf-Gueye et al., 1998) prior to addition of CT. The viability of the cells, tested by Trypan Blue exclusion, was always greater than 95%.

2.5. Real-time fluorescence and absorption measurements of drug transport in living cells

Fluorescence measurements were carried out using a Perkin Elmer LS50B spectrofluorometer equipped with a temperature-controlled sample compartment. Before the experiments, the cells were counted, centrifuged and resuspended in Hepes buffer. The appropriate concentration of CT was quickly added to the cuvette under magnetic stirring. Fluorescence intensity at 590 nm (excitation 470 nm) was measured continuously. During the time course of these experiments, aliquots were taken at various time intervals and used as such for flow cytometry measurements. A Becton Dickinson FACScan Flow cytometer equipped with a spectra Physics argon-ion laser was used. The fluorescence signal was gated on the forward angle light scatter signal to exclude dead cells debris from analysis. The argon-ion laser was tuned to 488 nm and used at a power of 15 mW. The emission was detected through an emission filter which collects radiations from 563 to 607 nm. The cells were not washed in order to minimize the re-equilibration of the fluorescent probe in the various intracellular compartments. Re-equilibration happens when probes from the extra-cellular medium are removed.

Absorption measurements were carried out using a Varian Cary 219 double beam spectrophotometer. Cells were treated as described above for the fluorescent measurements. Absorption spectra were recorded at various intervals of time.

2.6. DNA binding studies

Fluorescence spectroscopy and circular dichroism were used to monitor the interactions of CT with DNA. Absorption and circular dichroism measurements were made on a Jobin Yvon Model Mark CD-6 dichrograph. The instrument was calibrated using a standard solution of epiandrosterone (3.4×10^{-3}) in a 1 cm cell ($\Delta\varepsilon = 3.3\ M^{-1}\ cm^{-1}$ at 304 nm). All spectra were recorded using a 1 cm cell and the following parameters: λ = 280–700 nm, step 1 nm, speed 0.25 s, spectra bandwidth 2 nm, number of cycles 1. Water blanks were used as references.

Results were expressed as ε (molar absorption coefficient) and Δε (differential molar absorption coefficient). The values of ε and Δε were expressed as molar concentration of CT chromophore. Uncorrected fluorescence spectra were recorded at 37 °C on Perkin Elmer LS 50B spectrofluorometer.

3. Results

The CT structure and its NMR 13C spectrum are shown in the Fig. 1.

3.1. Time course of CT uptake by K562 and K562/ADR cells

Fig. 2A shows typical result obtained when K562 cells, 10^6/mL, either sensitive or resistant were incubated with 5 μM CT. The free CT has a low fluorescence signal at 590 nm (λ_{ex}=470 nm). Addition of sensitive cells showed a two-step variation of fluorescence intensity as a function of time: the first step (1) is an increase of fluorescence intensity during the first ~15 min, the second step (2) is a decrease of fluorescence intensity during the following ~100 min. However, the addition of resistant cells to a CT solution did not give rise to noticeable variation of the fluorescence intensity. These preliminary data already suggest that CT enters into sensitive cells but not resistant cells. To give further support to these data, sensitive cells were incubated for 15 min with CT in order to reach the end of step (1). Then cells were centrifuged and new sensitive cells were added to the supernatant. No increase of the fluorescence signal was observed. This shows that CT, which was formerly in solution, was absorbed by the cells during the first experiment. When the same protocol was performed with resistant cells, it was observed that the addition of sensitive cells to the supernatant of resistant cells yields a strong increase of the fluorescence signal. It proved that almost no CT has entered the resistant cells.

In a second set of experiments, resistant cells were first incubated for 30 min with 10 mM NaN_3, 5 mM deoxyglucose, in the absence of glucose. It is well-known that, under

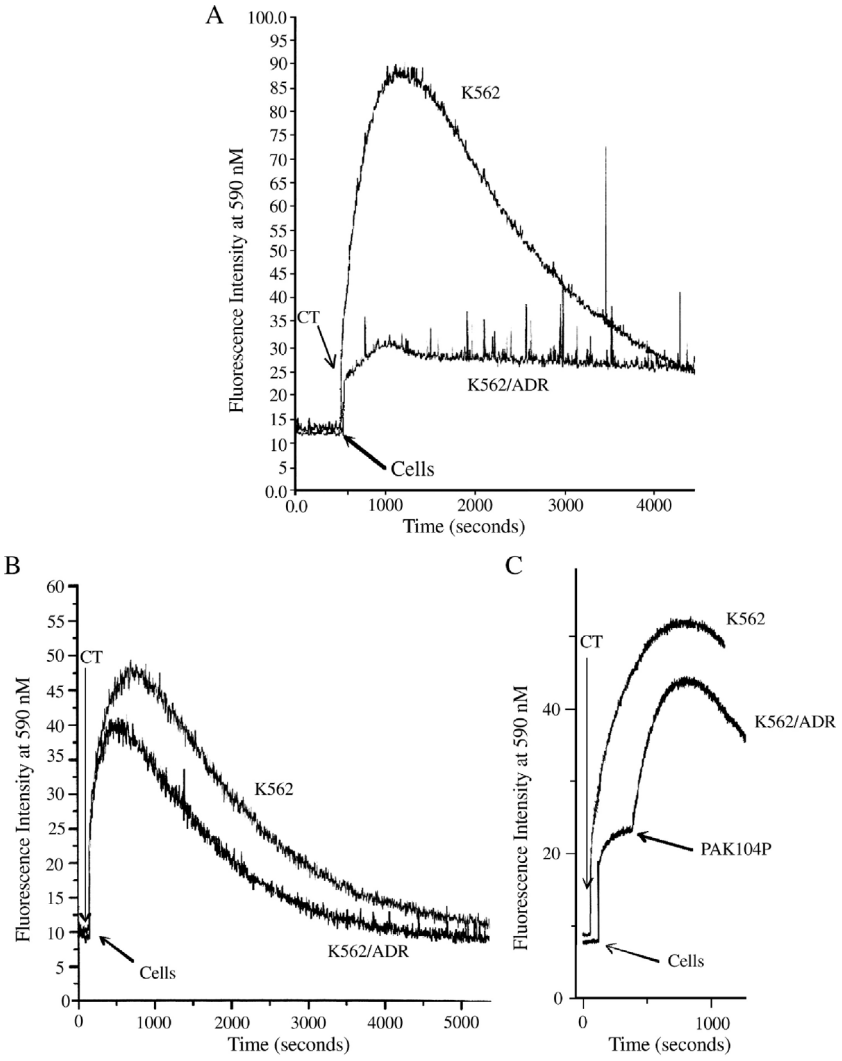

Fig. 2. Time course of carbazole thiazole (CT) uptake in K562 and K562/ADR cells. Cells (10^6/mL) were incubated at 37° with 5 μM CT. Fluorescence intensity at 590 nm (excitation 470 nm) was measured continuously as a function of time. The data points are from one representative experiment out of 4. (A) in Hepes buffer, (B) in Hepes buffer in the absence of glucose and presence of 10 mM NaN_3 plus 5 mM deoxyglucose, (C) in Hepes buffer in the presence of 10 μM PAK-104P.

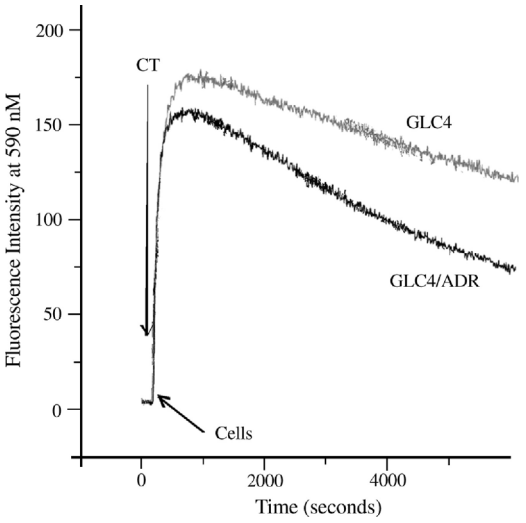

Fig. 3. Time course of carbazole thiazole (CT) uptake in GLC4 and GLC4/ADR cells. Cells (10^6/mL) were incubated in Hepes buffer at 37° with 5 μM CT. Fluorescence intensity at 590 nm (excitation 470 nm) was measured continuously as a function of time. The data points are from one representative experiment out of 4.

these experimental conditions, the ATP level is very low (Marbeuf-Gueye et al., 1998) and P-gp cannot pump out molecules from the cells. When CT was added to the energy-depleted K562/ADR cells, the same two steps variation of the fluorescence intensity as with sensitive cells were obtained. This treatment did not modify CT uptake in K562 cells (Fig. 2B).

In a third set of experiments, K562/ADR cells were incubated with 10 μM PAK-104P together with CT. The PAK-104P is a very efficient P-gp inhibitor (Marbeuf-Gueye et al., 2000). A two-steps variation of the fluorescence intensity similar to that of sensitive cells was obtained. This treatment did not modify CT uptake in K562 cells (Fig. 2C).

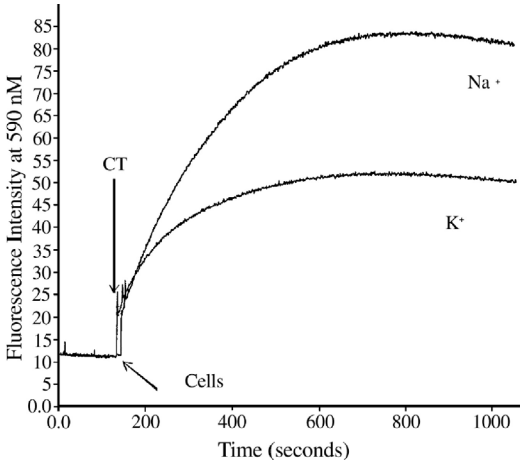

Fig. 4. Time course of carbazole thiazole (CT) uptake in K562 cells under conditions of decreased plasma membrane potential. 5 μM CT was added to cells (10^6/mL) suspended in either Na^+- or K^+-rich Hepes buffer at 37°. The data points are from one representative experiment out of 3.

These two last sets of experiments strongly support the assumption that in resistant cells, CT is pumped out by P-gp.

3.2. Time course of CT uptake by GLC4 and GLC4/ADR cells

The Fig. 3 shows a typical result when GLC4 cells, 10^6/mL, either cells which overexpress MRP1 (GLC4/ADR) or not (GLC4), were incubated with 5 μM CT. The uptake of CT by GLC4/ADR cells was slightly lower than what was obtained with sensitive ones. In both cases, a first increase of the fluorescent signal was followed by a decrease of this signal as in the case for K562 cells.

3.3. Time course of CT uptake by K562 cells under conditions of decreased membrane potential

The equalization of the intra- and extracellular concentrations of potassium was performed by incubating cells in Hepes buffer in which Na^+ was substituted by K^+ (135 mM). Such

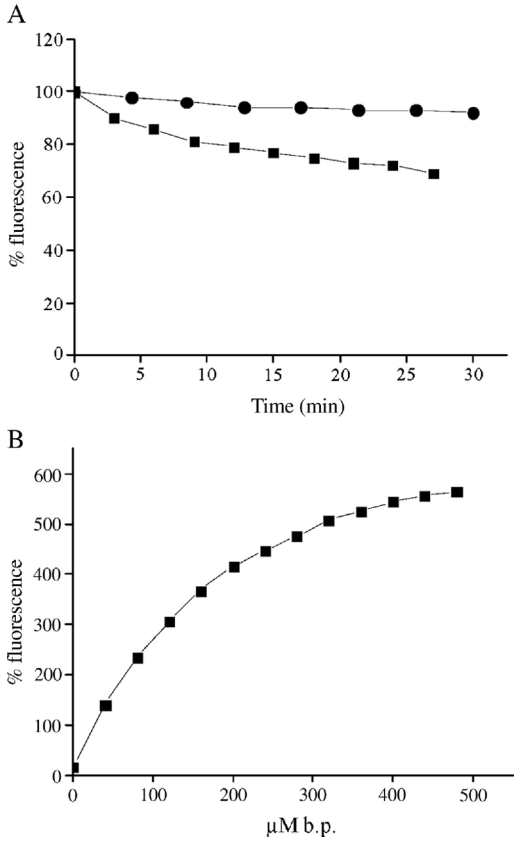

Fig. 5. (A) Interaction of carbazole thiazole (CT) with permeabilized cells or with isolated cell nuclei. The percentage of fluorescence intensity at 590 nm has been plotted as a function of time. (■) 5 μM CT was added to cells (10^6/mL) suspended in Hepes buffer at 37°, in the presence of 10 μl of triton X-100 4% to permeabilize plasma membrane. (●) 5 μM CT was added to nuclei isolated from cells (10^6/mL). (B) Fluorescence titration of carbazole thiazole (CT) interaction with DNA. DNA was stepwise added to 5 μM CT in Hepes at 37°. The fluorescence intensity signal is plotted as a function of the b.p. concentration. These experiments were performed twice. The data points are from one experiment.

experimental conditions almost completely depolarized the plasma membrane (Saengkhae et al., 2003). The Fig. 4 shows that under these experimental conditions CT uptake is higher in cells suspended in Na^+-rich buffer than in K^+-rich buffer. This proves that CT accumulation is sensitive to plasma membrane potential. It is expected as CT is a lipophilic cation.

In a second experiment, K562 cells (10^6 /mL) were allowed to accumulate CT in the presence of 1 μM FCCP, a protonophore, which is known to rapidly depolarize the mitochondrial membrane (Loetchutinat et al., 2003). The fluorescence signal was similar to that observed in the absence of FCCP. From this data one can infer that CT did not accumulate inside the mitochondria. It suggests that once inside the cytosol CT has a strong binding site and is therefore not available for accumulation inside mitochondria.

3.4. Time course of CT interaction with permeabilized cells and with isolated cell nuclei

The following experiments were designed to explain the two-step behavior of the fluorescence signal variation. In experiment 1, in order to permeabilize the plasma membrane, CT was added to either K562 or K562/ADR cells together with 10 μl of 4% Triton X-100. The fluorescence signal increased immediately and was followed by a slow decrease of fluorescence intensity similar to the second step (2) in intact cells (Fig. 5A). A similar result was obtained when cells were sonicated before the addition of CT: a fast increase of the fluorescent signal followed by a slow decrease (data not shown). In experiment 2, 5 μM CT was added to isolated cell nuclei suspended in Hepes buffer. The fluorescent signal increased at once to the value observed at the end of step one in sensitive cells and then maintained plateaued (Fig. 5A). These data strongly suggested that the increase of fluorescence intensity during step one was due to CT interaction with DNA in the nucleus.

3.5. Interactions of carbazole thiazole (CT) with DNA: spectral changes

These experiments were designed to determine if the increase in the fluorescence signal observed when cells were incubated with CT was due to its interaction with DNA.

3.5.1. Fluorescence spectral change

Free CT has a very low fluorescence signal at 590 nm (λ_{ex}=470 nm) and addition of DNA caused a large increase in fluorescence intensity. Fluorescence titration of 5 μM CT with DNA (0–100 μM b.p.) is shown in Fig. 5B. The fluorescence signal intensity reached a plateau for a [b.p.]/[CT] ratio ~100, and 50% of the signal increase was obtained for [b.p.]/[CT]= 20±4.

3.5.2. UV-visible absorption and CD spectral changes

Addition of DNA (0–600 μM b.p.) to CT resulted in a shift of the (50 μM) CT spectrum to longer wavelengths: the absorption band of CT at 456 nm moved to 480 nm. No noticeable modification of the extinction coefficient at the wavelength of this peak was observed (Fig. 6A). Free CT is not chiral and therefore does not exhibit CD signal. Addition of DNA gave rise to the appearance of a CD signal (Fig. 6B). Δε at 464 nm has been plotted as function of the [b.p.]/[CT] ratio value and 50% of the signal increase was obtained for [b.p.]/[CT]=2.0±0.4.

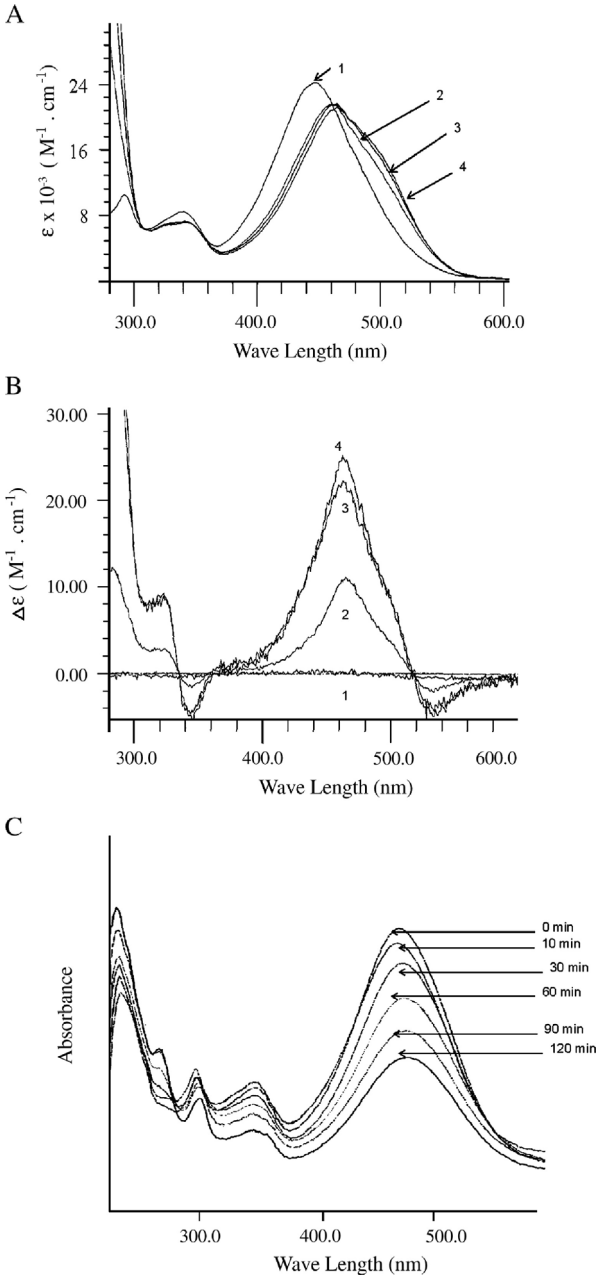

Fig. 6. Circular dichroism and absorption spectroscopy monitoring of carbazole thiazole (CT) interaction with DNA. Circular dichroism (A) and absorption (B) spectra of 30 μM CT in the presence of increasing amount of DNA, in Hepes buffer at 37 °C: [b.p.]/[CT] is equal to 0 in (1); 5 in (2); 9 in (3); 14 in (4). (C) Absorption spectroscopy monitoring of the interaction of carbazole thiazole (CT) with K562 cells. 5 μM CT was added to cells (10^6/mL) suspended in Hepes buffer at 37 °. The absorption spectrum was recorded after time intervals ranging from 0 to 120 min.

From these data, we can already assert that the first step (1), which is observed when CT is incubated with cells, is due to its interaction with DNA in the nucleus.

3.6. Time course of CT uptake by K562 cells monitored by absorption spectroscopy

The K562 cells (10^6/mL) were incubated in Hepes buffer at 37° with 5 μM CT and the absorption spectrum was recorded as a function of time (Fig. 6C). One observed a shift of the visible absorption band which occurred during the first ~20 min. This can be assigned to the uptake of CT by cells and its interaction with nucleus (step (1)). Then as time elapsed a decrease of the visible absorption band together with the appearance of a new band in the UV at ~250 nm was observed. About 50% of the signal modification was obtained after 1 h. We can already infer that these spectral modifications can be related to the second step (2). The decrease of the visible band, concomitantly with the appearance of a new one in the UV, is probably due to reduction of the ethylene double bond between the benzothiazolium and carbazole groups. It disrupts the electronic conjugation across the whole molecule. Under these conditions the absorption in the UV part of the spectrum arises from the carbazole moiety. Actually, the addition of 15 μM sodium dithionite to 4 μM CT gave rise, within ~1 h, to the disappearance of the 460 nm absorption band and the appearance of the 270 nm one.

3.7. Reaction of CT with intracellular reducing agents

These experiments aimed to determine which intracellular molecules were able to reduce CT. In the cytosol the most abundant reducing agents are glutathione GSH and NADH. The incubation of CT with 10 mM GSH did not give rise to any spectral modification. However, when similar experiments were performed with 90 μM NADH and 4 μM CT, in Hepes buffer at 37°, the CT visible absorption band decreased as time elapsed. This was concomitant with the appearance of the band at 270 nm. When 1 CT molecule was reduced, ~1.5 NADH molecules were oxidized.

4. Discussion

In developed countries the number of elderly people is growing rapidly and, therefore, an increase in neurodegenerative and cerebrovascular disorders causing dementia is expected. Alzheimer's disease is the most common cause of dementia. Early recognition and intervention helps optimal care of Alzheimer's patients. It delays the morbidity with this progressive illness (Chang and Silverman, 2004). Alzheimer's disease develops as a result of the progressive degeneration of specific pathways in the brain. β-amyloid is a major protein component of senile plaques in Alzheimer's disease, and is neurotoxic when aggregated (Selkoe, 2003). The size of aggregated β-amyloid responsible for the observed neurotoxicity and the mechanism of aggregation are still under investigation. However, prevention of fibril formation still holds promise as a mean to reduce β-amyloid neurotoxicity.

The development of molecules to be used as inhibitors of Alzheimer β-amyloid fibril formation was a goal of research for several years. Numerous series of compounds were described that effectively inhibit β-amyloid fibril formation. These include quaternary ammonium salts (Wood et al., 1996), sulphonates dyes (Sadler et al., 1995), nicotine (Salomon et al., 1996), rifamycins (Tomiyama et al., 1996), cyclodextrin (Camilleri et al., 1994), haemin (Howlett et al., 1997), anthracyclines (Gianni et al., 1995), curcumin (Yang et al., 2005), carbazoles (Howlett et al., 1999), cystatin C (Sastre et al., 2004). Most of these molecules are efficient *in vitro* but very few studies have been performed *in vivo* because of the poor passage of most of molecules through the blood brain barrier.

The blood brain barrier is located between the blood and the brain extracellular space, in the endothelial cells of brain capillaries joined by tight junctions (Ballabh et al., 2004). The blood brain barrier is a major impediment to the entry of many therapeutic drugs into the brain. A very significant number of molecules, including many useful therapeutic drugs, have lower brain permeability because these molecules are substrates for the ABC-transporters which are present in the brain capillary endothelial cells. These transporters efficiently remove the drug from the central nervous system, limiting drug brain uptake (Begley, 2004). The P-gp was the first of these ABC transporters to be described, followed by the MRP1, and more recently breast cancer resistance protein (BCRP). All are expressed in the blood brain barrier and combine to reduce the brain penetration of many drugs (Leslie et al., 2005; Amakrishnan, 2003). The P-gp and MRP1 are located in the luminal membranes of endothelial cells. The P-gp is involved in the efflux of many amphipathic cationic drugs while MRP1 extrudes neutral and anionic compounds (Scherrmann, 2005). Consequently, these ABC proteins help to protect the brain from the potential toxicity of exogenous compounds. Drugs targetting brain should be designed to overcome these mechanisms.

In the context of research on Alzheimer's disease, we are interested on the ability to go through the blood brain barrier of β-amyloid fibril formation inhibitors and β-amyloid markers (Darghal et al., 2006). As it was previously reported that carbazoles can inhibit β-amyloid fibril formation (Howlett et al., 1999), we wondered whether carbazoles would be able to pass the blood brain barrier and if these compounds would be substrates for P-gp and MRP1.

For this purpose, we have synthesized a carbazole derivative, carbazole thiazole, a slightly fluorescent compound which fluorescence is increased through interaction with cellular components. Thanks to this property, we were able to follow its evolution inside the cells.

The carbazole rings also present DNA binding properties. The binding affinity depends on the substitution of the carbazole ring (Sajewicz and Dlugosz, 2000). In some cases, (pyrimidyl groups), the affinity and the effects may be comparable to those obtained with doxorubicin (Tanious et al., 2000). Consequently, compounds derived from carbazole were proposed to be potential anticancer agents (Chang and Silverman, 2004). Some of the carbazole derivative may present fluorescence properties.

Our data show that the lipophilic cation carbazole thiazolium enters rapidly into the cells by passive diffusion and that its accumulation depends on the plasma membrane potential. Once inside the cell CT does not accumulate inside the mitochondria, as this could be expected, but binds to DNA in the nucleus, yielding a strong increase of the fluorescence signal. The binding of CT to DNA is fast. The limiting step in the increase of the fluorescence signal is the crossing of the molecule through the plasma membrane. The binding of CT to DNA was expected. It is well documented that carbazoles bind to DNA most of the time in the minor groove (Tanious et al., 2000). This is corroborated by our findings with isolated nuclei and DNA. In a second step CT is slowly reduced by probably NADH. This leads to the disappearance of the absorption band at 470 nm due to reduction of the double bond between carbazole and thiazole. Concomitantly, an absorption band appears at 260 nm, characteristic of unconjugated carbazole. Our data also show that CT is a good P-gp substrate as CT is not detected in P-gp-overexpressing cells. The addition of P-gp inhibitor allows CT uptake by these cells. However, CT is not an MRP1 substrate.

We conclude that even if carbazole derivatives are, *in vitro,* efficient in inhibiting β-amyloid formation, this efficiency could be highly compromised: being P-gp substrates they will probably not pass through the blood brain barrier. Of course this result should be corroborated using an *in vivo* model such as transgenic mice overexpressing β-amyloid.

Acknowledgements

We would like to thank the CNRS, Institut Fédératif de Recherche-Paris Plaine de France and University Paris 13 for financial support in the framework of the PPF-chimie program.

References

Abbott, N.J., 2002. Astrocyte–endothelial interactions and blood–brain barrier permeability. J. Anat. 200, 629–638.

Amakrishnan, P., 2003. The role of P-glycoprotein in the blood–brain barrier. Einstein Q. J. Biol. Med. 19, 160–165.

Ballabh, P., Braun, A., Nedergaard, M., 2004. The blood–brain barrier: an overview: structure, regulation, and clinical implications. Neurobiol. Dis. 16, 1–13.

Begley, D.J., 2004. ABC transporters and the blood–brain barrier. Curr. Pharm. Des. 10, 1295–1312.

Camilleri, P., Haskins, N.J., Howlett, D.R., 1994. Beta-cyclodextrin interacts with the Alzheimer amyloid beta-A4 peptide. FEBS Lett. 341, 256–258.

Chang, C.Y., Silverman, D., 2004. Accuracy of early diagnosis and its impact on the management and course of Alzheimer's disease. Expert Rev. Mol. Diagn. 4, 63–69.

Darghal, N., Garnier-Suillerot, A., Salerno, M., 2006. Mechanism of thioflavin T accumulation inside cells overexpressing P-glycoprotein or multidrug resistance-associated protein: role of lipophilicity and positive charge. Biochem. Biophys. Res. Commun. 343, 623–629.

Farrell Jr., R.E., 1998. Analysis of nuclear RNA. In: Farrell Jr., R.E. (Ed.), RNA Methodologies: A Laboratory Guide for Isolation and Characterization. Academic Press, San Diego, pp. 406–437.

Gianni, L., Bellotti, V., Gianni, A.M., Merlini, G., 1995. New drug therapy of amyloidoses: resorption of AL-type deposits with 4′-iodo-4′-deoxydoxorubicin. Blood 86, 855–861.

Howlett, D., Cutler, P., Heales, S., Camilleri, P., 1997. Hemin and related porphyrins inhibit beta-amyloid aggregation. FEBS Lett. 417, 249–251.

Howlett, D., George, A., Owen, D., Ward, R., Markwell, R., 1999. Common structural features determine the effectiveness of carvedilol, daunomycin and rolitetracycline as inhibitors of Alzheimer β-amyloid fibril formation. Biochem. J. 343, 419–423.

Leslie, E.M., Deeley, R.G., Cole, S.P.C., 2005. Multidrug resistance proteins: role of P-glycoprotein, MRP1, MRP2, and BCRP (ABCG2) in tissue defense. Toxicol. Appl. Pharmacol. 204, 216–237.

Loetchutinat, C., Saengkhae, C., Marbeuf-Gueye, C., Garnier-Suillerot, A., 2003. New insights into the P-glycoprotein-mediated effluxes of rhodamines. Eur. J. Biochem. 270, 476–485.

Lozzio, C.B., Lozzio, B.B., 1975. Human chronic myelogenous leukemia cell-line with positive Philadelphia chromosome. Blood 45, 321–334.

Marbeuf-Gueye, C., Broxterman, H., Dubru, F., Priebe, W., Garnier-Suillerot, A., 1998. Kinetics of anthracycline efflux from mutidrug resistance protein-expressing cancer cells compared with P-glycoprotein-expressing cancer cells. Mol. Pharmacol. 53, 141–147.

Marbeuf-Gueye, C., Salerno, M., Quidu, P., Garnier-Suillerot, A., 2000. Inhibition of the P-glycoprotein-and multidrug resistance protein-mediated efflux of anthracyclines and calceinacetoxymethyl ester by PAK-104P. Eur. J. Pharmacol. 391, 207–216.

Sadler, I.I., Hawtin, S.R., Tailor, V., Shearman, M.S., Pollack, S.J., 1995. Glycosaminoglycans and sulphated polyanions attenuate the neurotoxic effects of beta-amyloid. Biochem. Soc. Trans. 23, 106S.

Saengkhae, C., Loetchutinat, C., Garnier-Suillerot, A., 2003. Kinetic analysis of rhodamines efflux mediated by multidrug resistance protein (MRP1). Biophys. J. 85, 2006–2014.

Sajewicz, W., Dlugosz, A., 2000. Cytotoxicity of some potential DNA intercalators (carbazole, acridine and anthracene derivatives) evaluated through neutrophil chemiluminescence. J. Appl. Toxicol. 20, 305–312.

Salomon, A.R., Marcinowski, K.J., Friedland, R.P., Zagorski, M.G., 1996. Nicotine inhibits amyloid formation by the beta-peptide. Biochemistry 35, 13568–13578.

Sastre, M., Calero, M., Pawlik, M., Mathews, P.M., Kumar, A., Danilov, V., Schmidt, S.D., Nixon, R.A., Frangione, B., Levy, E., 2004. Binding of cystatin C to Alzheimer's amyloid beta inhibits in vitro amyloid fibril formation. Neurobiol. Aging 25, 1033–1043.

Scherrmann, J.M., 2005. Expression and function of multidrug resistance transporters at the blood–brain barriers. Expert Opin. Drug Metab. Toxicol. 1, 233–246.

Selkoe, D.J., 2003. Folding proteins in fatal ways. Nature 426, 900–904.

Tanious, F., Ding, D., Patrick, D., Bailly, C., Tidwell, R., Wilson, W., 2000. Effects of compound structure on carbazole dication-DNA complexes: tests of the minor-groove complex models. Biochemistry 39, 12091–12101.

Tomiyama, T., Shoji, A., Kataoka, K., Suwa, Y., Asano, S., Kaneko, H., Endo, N., 1996. Inhibition of amyloid beta protein aggregation and neurotoxicity by rifampicin. Its possible function as a hydroxyl radical scavenger. J. Biol. Chem. 271, 6839–6844.

Wood, S.J., MacKenzie, L., Maleeff, B., Hurle, M.R., Wetzel, R., 1996. Selective inhibition of Abeta fibril formation. J. Biol. Chem. 271, 4086–4092.

Yang, F., Lim, G.P., Begum, A.N., Ubeda, O.J., Simmons, M.R., Ambegaokar, S.S., Chen, P.P., Kayed, R., Glabe, C.G., Frautschy, S.A., Cole, G.M., 2005. Curcumin inhibits formation of amyloid beta oligomers and fibrils, binds plaques, and reduces amyloid in vivo. J. Biol. Chem. 280, 5892–5901.

Zijlstra, J.G., De Vries, E.G.E., Mulder, N.H., 1987. Multifactorial drug resistance in an adriamycin-resistant human small cell lung carcinoma cell line. Cancer Res. 47, 1780–1784.